New thick Silicon Carbide detectors: response to 14 MeV neutrons and comparison with single-crystal diamonds

M. Rebai[1,2], D. Rigamonti[1,2], S. Cancelli[3], G. Croci[2,3], G. Gorini[2,3], E. Perelli Cippo[1], O. Putignano[3], M. Tardocchi[1,2], C. Altana[4], M. Angelone[5], G. Borghi[6], M. Boscardin[6], C. Ciampi[7,8], G.A.P. Cirrone[4], A. Fazzi[9,10], D. Giove[10], L. Labate[11], G. Lanzalone[4], F. La Via[12,4], S. Loreti[5], A. Muoio[4], P. Ottanelli[7,8], G. Pasquali[7,8], M. Pillon[5], S.M.R. Puglia[4], A. Santangelo[13], A. Trifiro[14,15] and S. Tudisco[4]

[1]*Istituto per la Scienza e Tecnologia dei Plasmi Consiglio Nazionale delle Ricerche, Milano, Italy*
[2] *INFN sezione di Milano-Bicocca, Milano, Italy*
[3]*Dipartimento di Fisica 'G. Occhialini', Università di Milano-Bicocca, Milano, Italy*
[4] *Istituto Nazionale di Fisica Nucleare (INFN), Laboratori Nazionali del Sud (LNS), Via S. Sofia 62, 95123 Catania, Italy*
[5]*Associazione EURATOM-ENEA sulla Fusione ENEA C.R. Frascati, Via E. Fermi, 45, 00044 Frascati (Roma), Italy*
[6]*Trento Institute for Fundamental Physics and Applications (TIFPA), (INFN), Fondazione Bruno Kessler (FBK-Trento), Via Sommarive 14, 38123 Povo Trento, Italy*
[7]*INFN—Sezione di Firenze, Via G. Sansone 1, 50019 Sesto Fiorentino, Italy*
[8] *Dipartimento di Fisica, Università di Firenze, Via G. Sansone 1, 50019 Sesto Fiorentino, Italy*
[9]*Department of Energy of Politecnico di Milano, Via Lambruschini 4, 20156, Milano*
[10] *INFN-Sez Milano, Via Celoria 16, 20133 Milano*
[11]*Istituto Nazionale di Ottica, Consiglio Nazionale delle Ricerche, Via G. Moruzzi 1, 56124 Pisa, Italy*
[12]*Institute for Microelectronics and Microsystems, Consiglio Nazionale delle Ricerche VIII Strada, 5, 95121 Catania, Italy*
[13] *STMicroelectronics, Stradale Primosole, 50, 95121 Catania, Italy*
[14]*Dipartimento di Scienze MIFT dell'Universitá di Messina, V.le F. S. D'Alcontres 31, 98166 Messina, Italy*
[15]*INFN-Sez Catania, Via Santa Sofia, 64 - 95123 Catania*

Abstract

In this work we present the response of a new large volume 4H Silicon Carbide (SiC) detector to 14 MeV neutrons. The device has an active thickness of 100 µm (obtained by epitaxial growing) and an active area of 25 mm^2. Tests were conducted at the ENEA-Frascati Neutron Generator facility by using 14.1 MeV neutrons. The SiC detector performance was compared to that of Single-Crystal Diamond (SCD) detectors. The SiC response function was successfully measured and revealed a very complex structure due to the presence in the detector of both Silicon and Carbon atoms. Nevertheless, the flexibility in the SiC manufacturing and the new achievements in terms of relatively large areas (up 1x1 cm^2) and a wide range of thicknesses makes them an interesting alternative to diamond detectors in environments where limited space and high neutron fluxes are an issue, i.e. modern neutron cameras or in-vessel tokamak measurements for the new generation fusion machines such as ITER. The absence of instabilities during neutron irradiation and the capability to withstand high neutron fluences and to follow the neutron yield suggest a straightforward use of these detectors as a neutron diagnostics.

1. Introduction

The range of application of high band-gap solid state detectors is expanding in those environments where the high neutron flux is an issue, such as in the high-flux spallation neutron sources and in the thermonuclear fusion environment. An example of the former is the ISIS spallation neutron source (Didcot, U.K.)[1], where neutrons are produced by 800 MeV protons impinging on a heavy material. Being a pulsed neutron source, instant neutron flux can be very high, therefore the small-size and the fast response-time features of high band-gap solid state detectors make them an interesting solution to monitor and measure the neutron flux. Single-crystal Diamond (SCD) detectors have been characterized in the past [2][3][4] and they are currently installed at the ChipIr beam-line at ISIS as beam monitors [5]. ChipIr, built for measuring the Single Events Effects on electronic devices, is a fast neutron beam-line that directly faces the spallation target: the neutron flux exceeds 10^6 n/s·cm^{2}above 10 MeV and therefore dedicated fast-neutron detectors are still in development for the measurement of the neutron flux in the 1-800 MeV energy range and able to work at high rates (> 1 MHz).

As for thermonuclear fusion environments, it has been shown that SCDs can be used as excellent spectrometers for 14 MeV neutrons [6] and a SCD detector matrix has been installed, e.g., at JET (Joint European Torus) for the diagnosis of the plasma in the upcoming Deuterium-Tritium campaign [7]. Measurements performed with Deuterium (D) plasmas at JET have demonstrated that spectroscopy with a moderate energy resolution can also be performed [8][9] with 2.5 MeV neutrons. The limited availability of large size commercial single-crystal diamonds has led to the development of a 12-pixel (4.5 x 4.5 mm^2 each) matrix to boost the counting rate, especially in D plasmas, instead of having a single diamond detector with equal area.

Diamond detectors have been shown to withstand neutron fluence up to $2*10^{14}$ n/cm^2 as shown in [10] for single crystal and in [11] for polycrystalline diamonds. The latter, after irradiation with $8*10^{14}$ n/cm^2, recovers up to 70% of their initial performance after a suitable annealing. Moreover, transient effects have been noticed for SCD detectors irradiated with high energy neutrons and alpha particles [13][14]. Transient effects are due to partial trapping of the charge carries within the detector bulk defects and in the interfaces between the diamond crystal and the ohmic contacts. These are known as polarization effects and depend on the type, and amount, of crystal defects, naturally present or induced by neutron irradiation [15][16]. The polarization effect can be reset by inverting the bias voltage, as discussed in [14], but it could affect energy resolution if not accounted for.

In this paper we investigate the performance of new SiC detectors as an alternative to SCDs. SiC devices have been already used in the past to measure the thermal neutron flux in reactors [17] and the 14 MeV neutrons from DT reactions [18]. As shown in [19] good quality SiC detectors are now available and measurement of the fast neutron spectrum is possible also at high temperatures as done with diamond detectors [20].

The device used in present work was manufactured by SiCILIA (*Silicon Carbide detectors for Intense Luminosity Investigations and Applications*) [21] project which is a collaboration between IMM-CNR and INFN totally funded by INFN. The main goal of the project was the processes innovation and production of relatively large area SiC detectors for many applications [22][23][24][25][26][27], with thicknesses depending on the experiment requirements. Today, thanks to the SiCILIA R&D, SiC can be produced in relatively large areas (up to 1.5 cm^2) [28] and with thicknesses up to 250 µm which represent an excellent enhancement in the SiC growth technology. Moreover in the near future they could be worked in Geiger mode, in order to detect single photons [29][30].

Moreover, the possibility of growing SiC layers with large area and with different thickness, makes this material an interesting candidate for applications in fusion plasma physics, like for instance for Fast Ions Loss Detectors (FILD) that measure the fast ions lost by the plasma before they hit the first wall. Currently, FILD systems are based on scintillator crystals coupled to optical fibres leading scintillation light towards a CDD [12]. They work in an environment where neutrons are the highest source of background. An advantage of SiC in this application is that, by decreasing the crystal thickness, the detector efficiency for neutrons can be accordingly decreased to as low as 10^{-5}, without losing efficiency for 500 keV ions.

As in SCDs, neutron detection in SiC is based on the collection of electron-hole pairs produced by charged particles generated by neutron interaction with C and Si nuclei. Due to their abundances in natural C and Si, in this work we will consider only interaction on ^{12}C and ^{28}Si. This paper describes

measurements performed at the Frascati Neutron Generator (FNG) at Enea (Frascati, Italy) by using a SiCILIA SiC detector prototype and two SCDs with different thicknesses irradiated by 14 MeV neutrons. The SiC detector was irradiated up to a total fluence of $4.45*10^{11}$ neutrons/cm^2.
The paper is organized as follows: in Section 2 the neutron-induced reactions on ^{12}C and ^{28}Si are summarized and the detectors are compared in terms of construction parameters and features. In Section 3 the experiment performed at FNG is described, while in Section 4 the most important results will be illustrated.

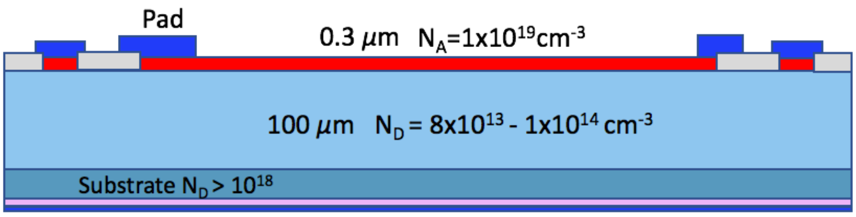

Figure 1 Cross section of the SiC detectors

2. The detectors

A. *Detectors production*

The SiC detectors were designed and manufactured at the CNR-IMM (Institute for Microelectronics and Microsystems) in Catania, starting from the growth of thick 4H epitaxial layers on four inch 4H-SiC wafers by means of a CVD (Chemical Vapour Deposition) process. During this phase dopants are provided by means of gaseous precursors such as N_2 for n-type doping and $Al_2(CH_3)_6$ (Trimethylaluminium) for p-type doping in order to realize p-n junction devices. The process was performed at a low-pressure and high temperature (1630 °C) regime.
The wafers were subsequently treated with several photolithographic steps, a first photolithography for the definition of the detector area by Inductive Coupled Plasma (ICP) etching was performed. Then, a second lithography was performed for the construction of the edge structures, aimed at reducing the electrical field at the device borders. The process continues with the deposition of an isolation oxide and the opening of the contacts with a further photolithographic process and a subsequent annealing to perform a good electric contact on p^+ region. Along the border of the active area of the detector a 200nm layer of Ti and Al was deposited in order to obtain a region well-suited for ultrasonic micro-bonding. Finally, the ohmic contact was formed by Titanium/Nickel/Gold deposition. A cross-section of the SiC detector used for the neutron measurements described in this paper is shown in Fig.1. It features a 300 nm thick p-layer with a doping concentration $N_A=1x10^{19}cm^{-3}$ and a 100 μm thick n-layer with a doping concentration, N_D, between $8x10^{13}cm^{-3}$ and $1x10^{14}$ cm^{-3}. The detector has an active area of about 10x10 mm^2, segmented in four regions of 5x5 mm^2, and was mounted on a PCB board (Figure 3 A) designed to be housed in an aluminium box.
The SCD detectors were designed and built at the CNR-IFP (Institute of Plasma Physics) in Milan and at the CNR-ISM institute in Rome (Italy) [31][32][33]. The first SCD is made of a single-crystal diamond sample (4.5*x*4.5*x*0.5mm^3) grown with a CVD technique with boron concentration [*B*] <5 ppb and nitrogen concentration [*N*] <1 ppb), provided by Element Six Ltd. [34]. The second, equal to the first one, has been thinned by laser cutting to a layer thickness of 150 μm. Ohmic contacts were obtained on the top and bottom surfaces of the samples by subsequent sputtering depositions of a multilayer metal structure (patent pending), followed by a final gold layer deposition, in order to improve weldability with microwires and to prevent oxidation of the underlying structure. The

contact thickness is 200 nm with a lateral dimension of 4.2*x*4.2mm^2. A dedicated 1mm thick alumina Printed Circuit Board (PCB) was designed and fabricated; the bottom surfaces of the diamond samples were glued with a thin layer of conductive silver paste on the pad, whereas the top surfaces were wire-bonded (by means of 25 μm thick Al/Si wires) on the ground plane. The alumina PCB is housed inside a properly designed aluminium metal case in order to shield it from electromagnetic interference and to give the detectors the mechanical resistance necessary for handling.

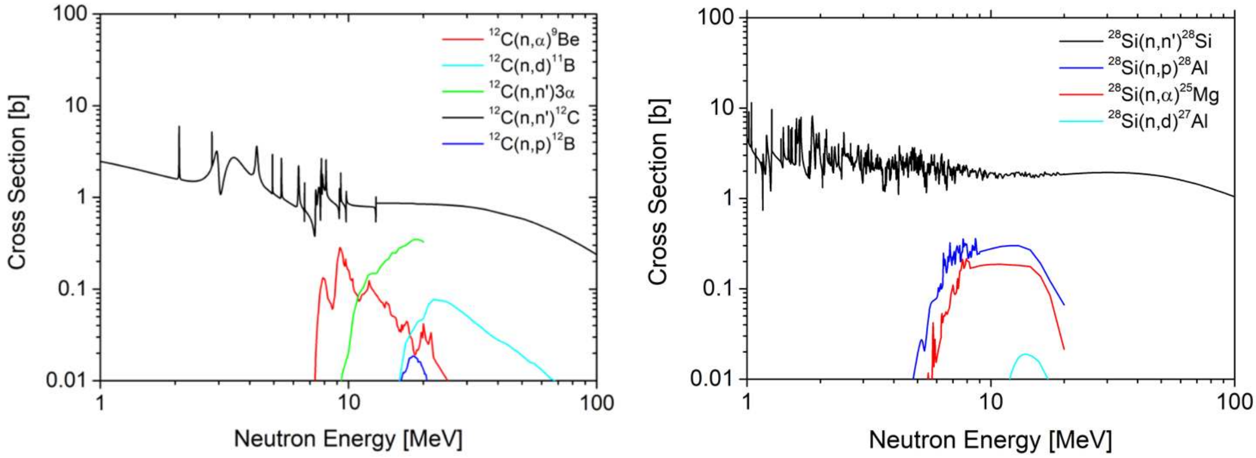

Figure 2 Cross sections for neutron interaction on Carbon (left) and on Silicon (right). Data from the ENDF/B-VI.0 for ^{12}C and ENDF/B-VIII.0 for ^{28}Si***[35].***

A. *Neutron detection*

Neutron detection is based on the collection of the electron-hole (e-h) pairs produced by neutron interaction with ^{12}C in SCDs and with both ^{12}C and ^{28}Si in SiC detectors. The most important reactions induced by neutrons in the MeV energy range on Carbon and Silicon are reported in Table 1 and their cross-sections in Figure 2. The most relevant neutron-induced process in both Carbon and Silicon is the *elastic scattering* (black lines in Figure 2), in which only a fraction of the neutron energy is released into the detector, by means of the energy of the recoiling atom, given by $E_d=E_n*\cos\theta(4A)/(1+A)^2$, where E_n is the incoming neutron energy, θ is the recoil angle and A the mass number of the recoiling atom. The maximum energy that can be released into the detector is $E_{d,max}$=4.00 MeV and $E_{d,max}$=1.87 MeV for recoils of Carbon and Silicon ions, respectively. All the energy values smaller than $E_{d,max}$ can possibly be released by this process into the detector; as a consequence, a typical edge-type shape is produced into the Pulse Height Spectrum (PHS) of the detector. Concerning the reactions $^{A}X(n,\alpha)^{A-3}Y$ and $^{A}X(n,p)^{A}Y$, being two-body reactions, all the neutron energy minus the reaction Q-value is deposited into the detector.

Table 1: Main 14 MeV neutron-induced reactions on Carbon and Silicon. For each reaction, the threshold, the Q-value and the position of the peak in the PHS are given. The last column is the label of the peak observed in the experimental PHS shown in ***Figure 6***. If the nucleus is left in an excited state the energy which can be released into the detector is given for the first nine excited states.

Reaction	Threshold	Q_{value} [MeV]	E_d [MeV]	Label
^{12}C(n,n) ^{12}C	-	-	$E_{d,max}$=4.0	0
^{12}C(n ,α)^{9}Be	6.2	-5.702		
	Ground state		8.398	1
	1st excited state		6.761	
^{12}C(n,p)^{12}B	13.645	-12.587		
	Ground state		1.513	
	1st excited state		0.56	

$^{12}C(n,n')3\alpha$	7.886	-7.275	6.825	2
$^{28}Si(n, n)\,^{28}Si$	-	-	$E_{d,max}$=1.87	
$^{28}Si(n, \alpha)\,^{25}Mg$	2.749	-2.654		
	Ground state		11.446	3a
	1st excited state		10.861	3b
	2nd excited state		10.471	3c
	3rd excited state		9.834	3d
	4th excited state		9.481	3e
	5th excited state		8.644	3f
	6th excited state		8.041	3g
	7th excited state		8.032	3h
	8th excited state		7.538	3i
	9th excited state		7.475	3j

3. Experimental set-up

The response function of both SCDs and of the SiC detector, together with their neutron resistance and stability, has been investigated by irradiating the detectors with 14.1 MeV neutrons at FNG. Here, neutrons are produced by Deuterium-Tritium (DT) reactions obtained from deuterium ions accelerated up to 300 keV impinging on a tritiated-titanium target [36]. The detectors were placed at 90 degrees with respect to the beam direction (see Figure 3) at a distance between 13 and 18 cm from the target. The expected neutron spectrum at the detector position, calculated through MCNP simulations [37], features a main component, peaked at 14.1 MeV with a 130 keV broadening and a scattered neutron component at lower energies (see Figure 4).
During the measurements, the FNG neutron yield has been monitored as a function of time by the standard FNG monitor which detects the alpha particles produced by the DT reactions in the target.

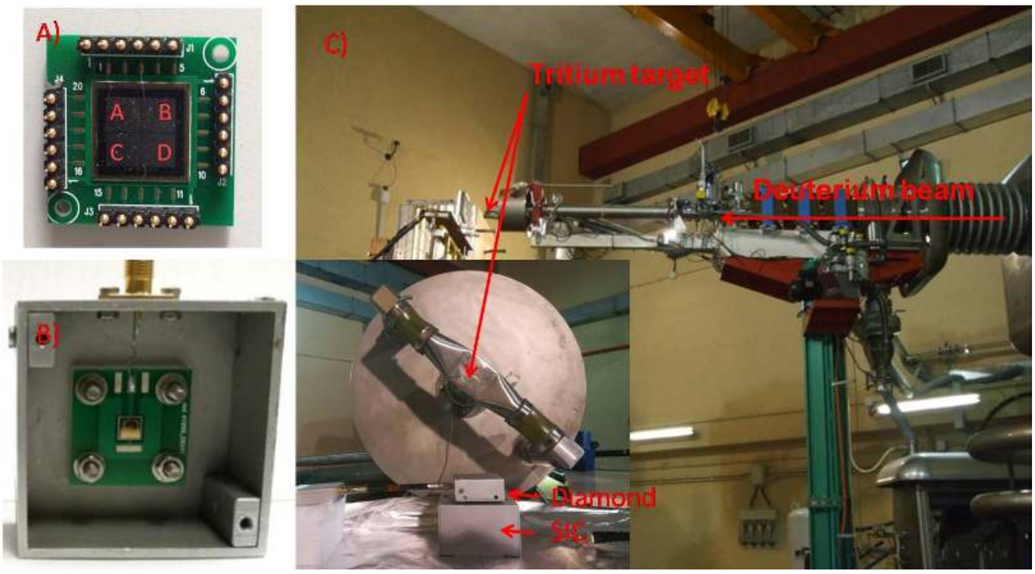

Figure 3 Pictures of the Silicon Carbide (A) and Single-crystal Diamond (B) detectors and their installation at the FNG facility (C). The SiC detector used for the measurement was the one labelled "A" in the top left panel.

A dedicated custom electronic chain was used to bias and collect charge carriers from each detector. In particular, the SCDs were coupled (through a 5 cm RG62 cable) to a CIVIDEC C6 fast charge preamplifier [38] with rise time of 3.5 ns and a shaping time of 25 ns. Signals were directly fed into a CAEN DT5730B digitizer (500 MSample/s and 14 bits) equipped with CAEN software able to perform on-line measurements of the pulse area [39].

The SiC spectrometer was connected to an ORTEC 142A preamplifier [40] with nominal decay time of 500 μs; the signal from it was fed into an ORTEC 570 amplifier [40] which provided a gain factor of 1000 and a shaping time of 1 μs. Finally, the signal was recorded and analysed in amplitude by a MAESTRO multi-channel analyser (MCA) [40]. Alternatively, for some measurements, the SiC was preamplified by a CX-L CIVIDEC spectroscopic amplifier producing a Gaussian output signal of 180 ns FWHM [38] and then directly digitized by the CAEN DT5730B.
Both the SCDs and the SiC detectors were biased by a CAEN NDT1470 [39] HV Module. A bias voltage V_{bias} equal to +400V and +120V was used to polarize the 500 μm and the 150 μm thick SCDs, respectively, giving rise to a constant electric field in the whole SCDs bulk of 0.8V/μm. A V_{bias} equal to -400V was used to polarize the SiC creating a depletion region of 73 μm.

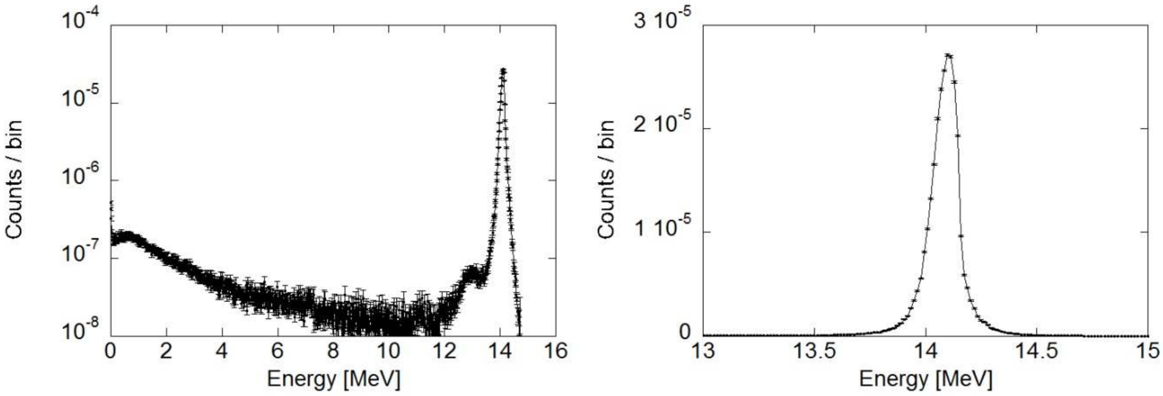

Figure 4 FNG Neutron spectrum expected at the SiC position. The spectrum, reported in logarithmic (left) and linear (right) scale, is peaked at 14.1 MeV with a 130 keV broadening.

4. **Measurements with 14 MeV neutrons**

The PHS measured with the two SCDs (Figure 5) feature the characteristic structures of neutron interaction with Carbon described in Section 2. A prominent peak, due to the $^{12}C(n,\alpha)^{9}Be$ reaction, is clearly visible at 8.4 MeV. This peak features a FWHM of 203 keV and 191 keV for the two SCDs (500 and 150 μm), respectively: taking into account the 130 keV FWHM of the beam, an energy resolution of 1.84% and 1.67% for the 500 μm and the 150 μm diamond has been obtained, respectively. At lower energies, three edges can be observed. The one at 6.8 MeV is due the carbon break-up reaction into three α particles, $^{12}C(n,n')3\alpha$. The edge at 4 MeV is due to the elastic recoil on ^{12}C, while the structure between 2.7 MeV and 3.3 MeV is due to a combination of *i)* elastic recoil at higher recoiling angles, ii) elastic recoil leaving carbon in the first excited state and *iii)* the carbon break-up reaction. Although, the two SCDs show a very similar PHS shape, a clear discrepancy between the two SCDs is observed in the lower energy part of the spectrum. This discrepancy, also visible in the (n,α) peak, is still under investigation and it could be due to the "wall" effect [41] related to the different diamond thickness.
If the PHS are observed in logarithmic scale, a peak at 10.3 MeV is clearly visible above the background. This peak is due to the $^{13}C(n,\alpha)^{10}Be$ reaction, which has a lower Q-value (-3.83 MeV) with respect to the (n,α) reaction on ^{12}C. Its intensity is limited to 0.5% of the (n,α) peak on ^{12}C by both its lower cross-section and the low natural abundance of ^{13}C (1.1%). These events limit the SCDs sensitivity on the high energetic ions in DT plasmas to about 10^{-2} with respect to main bulk emission as mentioned in [42].
The SiC PHS shows a more complicated structure due to the presence of the ^{28}Si, in particular, neutron interaction via (n,α) and (n,p) reactions on ^{28}Si can leave the ^{25}Mg and ^{28}Al nuclei on either

the ground state or the first excited states with different finite probabilities. This results in a number of peaks in the PHS that, together with the neutron-induced reactions on ^{12}C, give the spectra in Figure 6. The most important structures in the PHS have been labelled as in Table 1 in order to improve the comprehension of the spectrum. The most intense peak is placed at E_d=8.4 MeV and it is related to the (n,α) reaction on ^{12}C on the ground state. The same reaction channel on ^{28}Si can be observed at E_d=11.4 MeV. The intensity of this peak is limited with respect to the one occurring on ^{12}C because the (n,α) reaction can produce ^{25}Mg in an excited energy level (contributions corresponding to excited levels up to the 9^{th} can be recognized in Fig.6).

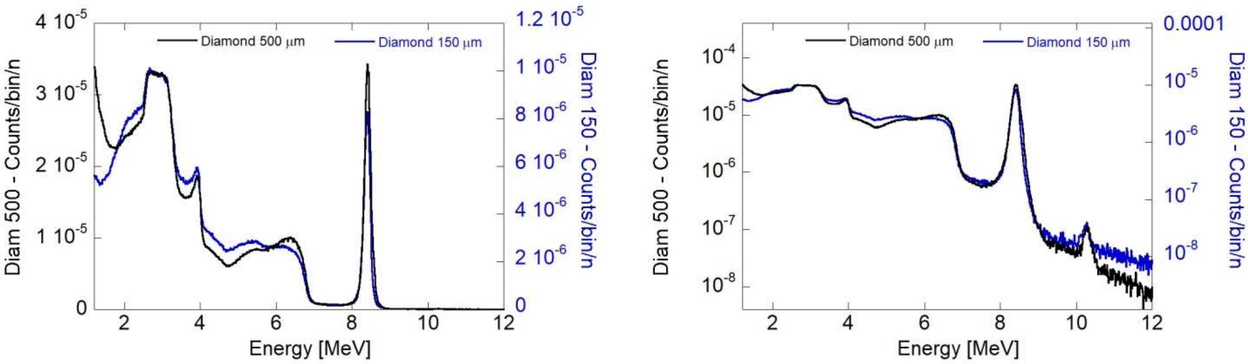

Figure 5 PHS for the 150µm thick diamond (blue line) and the 500 µm thick diamond (black line) in linear (left) and log scale (right). The left Y-axis refers to the spectrum obtained with the 500 µm SCD, while the right one refers to the 150 µm thick SCD. The spectra have been normalized with respect to the neutron fluence ($1.1 \pm 0.2 *10^{10} n/cm^2$ for the 500 µm diamond $2.6 \pm 0.4*10^{10} n/cm^2$ for the 150 µm diamond) and to the bin width is equal to 22 keV.

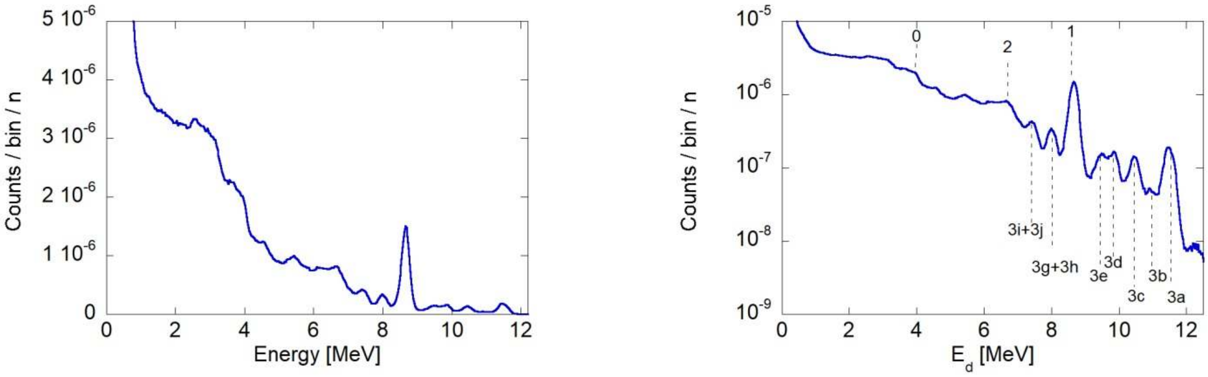

Figure 6 Pulse Height spectrum for the SiC in linear and log scale obtained with the ORTEC 142A preamplifier and 570 amplifier. The spectra have been normalized with respect to the neutron fluence ($2.4 \pm 0.3*10^{10} n/cm^2$) and the bin width is 22 keV. The labels in the log scale spectrum refer to the different reactions summarized in ***Table 1***.

At lower deposited energies the elastic edge on ^{12}C, placed at E_d=4 MeV is still visible, but the same interaction channel on ^{28}Si, which should be placed at 1.87 MeV, cannot be distinguished from the background. The (n,α) peaks feature a FWHM of 265 keV for the reaction $^{12}C(n,\alpha)^9Be$ and 365 keV for $^{28}Si(n,\alpha)^{25}Mg$ when ^{25}Mg is produced in the ground state: taking into account the beam energy FWHM of 130 keV, an energy resolution of 2.7% and 3% has been obtained respectively for the two peaks. The energy resolution achieved is good enough for measuring the temperature in ohmic plasmas [43] where an energy resolution better that 5% is required.

Besides the energy resolution and the sensitivity of the (n,α) peak to high energy components of the neutron spectrum, a crucial feature for neutron detectors is their efficiency. Two parameters can be used to assess the efficiency: the overall counts above a certain energy threshold and the counts corresponding to a specific reaction channel. Both methods have been used in this work. The threshold used for the evaluation of the efficiency has been chosen equal to E_d=1.2 MeV for all the detectors in order to discard the gamma-ray background and the counts due to electronic noise. The reaction channel used to compare the efficiency is the $^{12}C(n,\alpha)^{9}Be$ reaction producing the only peak in common between the two kind of detectors. The measured efficiency is here compared with the results of GEANT4 simulations giving the results shown in shown in Table 2.

Detector	Atomic/ molecular density [cm^{-3}]	Detector volume [cm^3]	Efficiency measured for E_d> 1.2 MeV [and normalized per atom]	Simulated efficiency for E_d> 1.2 MeV [and normalized per atom]	Efficiency measured in the $^{12}C(n,\alpha)^{9}Be$ peak	Simulated efficiency in the $^{12}C(n,\alpha)^{9}Be$ peak
SCD 500 μm	$1.76*10^{23}$	$1.0125*10^{-2}$	$(5.32 \pm 0.87) *10^{-3}$ [$2.98 *10^{-24}$]	$5.2 *10^{-3}$ [$2.92 *10^{-24}$]	$(3.98 \pm 0.73) *10^{-4}$	$5.45 *10^{-4}$
SCD 150 μm	$1.76*10^{23}$	$3.0375*10^{-3}$	$(1.59 \pm 0.25)*10^{-3}$ [$2.97 *10^{-24}$]	$1.6 *10^{-3}$ [$2.99 *10^{-24}$]	$(0.91 \pm 0.15) * 10^{-4}$	$1.47 *10^{-4}$
SiC 100 μm	$4.8*10^{22}$	$2.5*10^{-3}$	$(5.69\pm 0.78) *10^{-4}$ [$4.74 *10^{-24}$]	$6.73*10^{-4}$ [$5.61 *10^{-24}$]	$(2.02 \pm 0.30) *10^{-5}$	$2.73*10^{-5}$

Table 2 Efficiency measured and simulated for the three detectors for E_d>1.2 MeV and in the $^{12}C(n,\alpha)^{9}Be$ peak (note that for E_d>1.2 MeV the efficiency per atom is reported in square brackets). The error on the measured efficiency is the combination of the statistic error, a 5% uncertainty on the measure of the neutron fluence and a 5% uncertainty due to the subtraction of the background. Together with the values of the efficiency the detector volume and atomic/molecular density are reported.

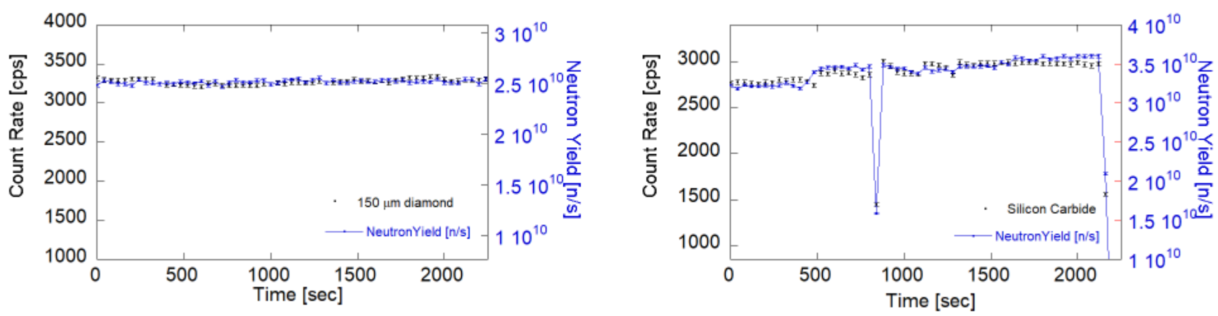

Figure 7 150 μm diamond (left) and SiC (right) detector counting rate compared to FNG neutron yield, both binned every 40 seconds. Note that the plots are in double Y scale: the left axis refers to the detectors counting rate while the right one refers to the neutron yield. The scale ratio between Y_{max} and Y_{min} is equal to 4 for all the plots.

The most efficient detector among the ones examined is the 500 μm-thick diamond; this is due to the fact that the probability of neutron interaction scales with the volume of the detector and the material atomic density. The agreement between the simulated and the measured efficiency is rather good in all the considered cases especially for the overall efficiency. Moreover, the efficiency normalized to atom number indicates that the two SCD detectors behave the same when irradiated with fast neutrons; on the other hand, the higher normalized efficiency of the SiC reflects the higher neutron reaction cross section on Silicon.

The measured efficiency for the $^{12}C(n,\alpha)^{9}Be$ peak is always lower than the simulated one. This could be due to events with only a partial charge collection efficiency not contributing to the main peak.

It could also be due to discrepancies between the $^{12}C(n,\alpha)^{9}Be$ reaction cross section employed in the simulation and the actual one.

Together with the efficiency evaluation, the stability of the detectors compared to the total FNG neutron yield was measured. The FNG neutron yield, monitored during the irradiation of all the detectors, showed a very good agreement in terms of counting rate with all the detectors (Figure 7). The Pearson correlation coefficients were calculated for the two detectors being equal to 0.9793 and 0.9770 for the diamond and the SiC respectively.

5. **Conclusion**

The Silicon Carbide detector produced within the SiCILIA project has been tested at FNG by using 14.1 MeV neutrons. The detector, featuring an active area of 25 mm^2 and an epitaxial thickness of 100 μm, showed good efficiency values thus demonstrating the improvements made in the growing procedures. The absence of instabilities during neutron irradiation up to a 14 MeV neutron fluence of $4.45*10^{11}$ n/cm^2 suggests a straightforward use of this detector as a fast neutron diagnostic. The Pulse Height spectrum obtained from the SiC detector revealed a very complex response function due to the presence of both ^{12}C and ^{28}Si. This complexity limits the sensitivity of the SiC when used as a neutron spectrometer for Deuterium-Tritium plasma diagnostics [7][42], though it could be well suited to measure the temperature in thermal plasmas. Furthermore, it could be successfully used as a neutron diagnostic in those environments in which small size is a requirement, such as in a neutron camera. In addition, the possibility of growing Silicon Carbide layers with different thicknesses allows for tuning the neutron detection efficiency, and, therefore, using SiC crystals as charged particle detectors in those environments where high neutron fluxes are an issue, such as in FILD detectors.

This work is the first step towards the realization of a fast neutron detector based on Silicon Carbide. More measurements are planned in order to measure the SiC detector response function to neutrons of different energies as already done for diamond based detectors [45] and to assess the detector radiation hardness as done in [10] with diamonds. The present work shows that the Silicon Carbide detector is able to withstand 14 MeV neutron irradiation without changing its performances which is of particular relevance in the case of the future nuclear fusion machines, such as ITER [46].

Acknowledgments

The work leading to this publication was funded by the INFN-Group 5 (Technology Research) and by EuroFusion-WP-JT60SA. The views and opinions expressed herein do not necessarily reflect those of Eurofusion and INFN.

References

[1] https://www.isis.stfc.ac.uk/
[2] M. Rebai et al., Journ. of Instrum 7 C05015 (2012). doi:10.1088/1748-0221/7/05/C05015
[3] M. Rebai et al., Nucl. Phys B 215, 313-315, 2011; doi:10.1016/j.nuclphysbps.2011.04.041
[4] C. Cazzaniga et al., JINST 11 P07012 (2016)
[5] C. Cazzaniga and C. D. Frost, Journal of Physics: Conference Series, Vol. 1021, conference
[6] D. Rigamonti et al., Meas. Sci. Technol. 29 045502

[7] L. Giacomelli et al., Rev. Sci. Instrum 87, 11D822 (2016); doi: 10.1063/1.4960307.
[8] M. Rebai et al., Rev. Sci. Instrum. 87, 11D823 (2016); doi: 10.1063/1.4960490
[9] A. Muraro et al., Rev. Sci. Instrum 87, 11D833 (2016); doi: 10.1063/1.4961557
[10] M. Pillon et al., Journal of Applied Physics 104, 054513 (2008)
[11] M. Angelone et al., Rev. Scient. Instrum 77, 023505 (2006)
[12] M. García-et al, Nucl. Fus. 47, 7 (2007)
[13] C. Cazzaniga et al., Nuclear Inst. and Methods in Physics Research, B 405 (2017) 1-10
[14] M. Rebai et al., Diamond & Related Materials 61 (2016) 1–6, DOI: 10.1016/j.diamond.2015.11.002
[15] Tanaka T. Tanaka et al., Diamond & Related Materials 14 (2005), 2031 -2034
[16] A. Lohstroh et al., Diamond & Related Materials 19 (2010) 841-845
[17] Frank H. Ruddy, et al., (2002) Radiation Detectors, Nuclear Technology, 140:2, 198-208
[18] Frank H. Ruddy, et al., IEEE TRANSACTIONS ON NUCLEAR SCIENCE, VOL. 53, NO. 3, JUNE 2006
[19] D. Szalkai, et al., Animma2015-283
[20] M. Angelone et al., (2017) 2016 IEEE Nuclear Science Symposium, Medical Imaging Conference and Room-Temperature Semiconductor Detector Workshop, NSS/MIC/RTSD 2016, 2017-January, art. no. 8069929
[21] A. Muoio et al., Eur. Phys. Jour., Web of Confer. 117, UNSP 10006 (2016)
[22] D. Carbone et al. Jour. of Phys. Conf. 312, 082016 (2011)
[23] G. Cristoforetti et al. Plasma Phys. and Contr. Fus. Vol. 56, iss. 9, n° 095001 (2014)
[24] D. Mascali et al. Rad. Eff. And Def. in Sol., 165, 730-736 (2010)
[25] D. Mascali et al. Eur. Phys. Lett., 100, 45003 (2012)
[26] L. Lanzanò et al. Euro. Biophys. Jour. with Biophys Lett., 36, 823-829 (2007)
[27] M. Lacognata et al. Phys. Lett. B, 664, 157-161 (2008)
[28] S. Tudisco et al., Sensors, 18, 2289 (2018)
[29] M. Mazzillo et al. Sens. and Actuators A-Phys, 138 306-312 (2007)
[30] P. Finocchiaro et al. Jour. of Mod. Optics, 54 199-212 (2007)
[31] D. M. Trucchi, et al.,IEEE Electron Device Lett. 33, 615–617 (2012)
[32] M. Girolami et al., IEEE Electron Device Lett. 33, 224–226 (2012).
[33] D. M. Trucchi et al., Diamond Relat. Mater. 14, 575–579 (2005).
[34] See http://www.e6.com for Element Six Ltd.
[35] https://www-nds.iaea.org/exfor/exfor.htm
[36] M. Angelone et al., Rev. Sci. Instrum. 67 (1996) 2189]
[37] https://mcnp.lanl.gov/
[38] www.cividec.at
[39] www.caen.it
[40] www.ortec-online.com
[41] G.F. Knoll,"Radiation detection and measurement"
[42] C. Cazzaniga et al., Rev. of Sci. Instrum. 85, 11E101 (2014); doi: 10.1063/1.4885356
[43] W. R. Faust and E. G. Harris, Nucl. Fusion **1**, 62 (1960).
[44] C. Cazzaniga et al., Rev. of Sci. Instrum. 85, 043506 (2014); doi: 10.1063/1.4870584
[45] M. Rebai et al., Journal of Instrum 8 P10007 (2013); doi:10.1088/1748-0221/8/10/P10007
[46] https://www.iter.org/